Available online at www.sciencedirect.com
SCIENCE DIRECT®
Ultrasonics xxx (2006) xxx–xxx
Ultrasonics
www.elsevier.com/locate/ultras

Fine grains ceramics of PIN–PT, PIN–PMN–PT and PMN–PT systems: Drift of the dielectric constant under high electric field

M. Pham-Thi [a,*], C. Augier [a,b], H. Dammak [b], P. Gaucher [b]

[a] Thales Research and Technology France, Domaine de Corbeville, 91404 Orsay Cedex, France
[b] Laboratoire Structures, Propriétés et Modélisation des Solides, UMR 8580 CNRS, Ecole Centrale de Paris, 92295 Châtenay-Malabry, France

Abstract

Lead-based ferroelectric ceramics with $(1-x)Pb(B_1\ B_2)O_3$–$xPbTiO_3$ formula have emerged as a group of promising materials for various applications like ultrasonic sonars or medical imaging transducers [Y.H. Chen, K. Uchino, J. Appl. Phys. (2001) 3928–3933]. $(1-x)$PMN–xPT, $(1-x)$PIN–xPT and ternary solutions xPIN–yPMN–zPT ceramics are synthesised using the solid state reaction method [Y. Hosono, Y. Yamashita, H. Sakamoto, N. Ichinose, Jpn. J. Appl. Phys. 42 (2003) 5681–5686]. Our objective is to achieve higher structural transition temperatures than those of PMN–PT ceramics with as good dielectric, piezoelectric and electromechanical properties. Ceramics capacitance and loss tangent are measured when the ac field of measurement increases up to $E = 0.5$ kV/mm. Behaviours of these materials under ac field are related to their coercive field and Curie temperature.

Keywords: Piezoelectric ceramic; PIN; PMN; PT; Non linear properties

1. Introduction

Complex perovskite so called relaxor $Pb(B_1B_2)O_3$ (B_1 = Mg, In, Sc...,Yb; B_2 = Nb, ...) (PMN, PIN, PSN) and $PbTiO_3$ (PT) show high piezoelectric properties especially for compositions near the morphotropic phase boundary (MPB) [1–3]. Such complex perovskites are of greater interest for electronic ceramic devices, piezoelectric actuators, underwater and medical acoustic transducers. Single crystals [4] and ceramics [5] of PIN–PT, PIN–PMN–PT were investigated. Phase transitions of PIN–PT system were established by temperature dependence of dielectric constant [6] and X ray diffraction [7]. It has been reported that the PIN–PT system has a MPB zone near $x = 37$, which separates a rhombohedral zone for low PT concentrations from a tetragonal zone for high PT concentrations [7]. The PIN–37PT composition, showing two structural transitions at $T_{MT} = 140$ °C between two ferroelectric phases and at $T_C = 300$ °C, exhibits good properties: $P_r = 0.344$ C/m^2, ε_{33}^T(@1 kHz) = 2670, $k_p = 57\%$ and $k_t = 47\%$.

This paper reports a study of PIN–PT and PIN–PMN–PT ceramics and compares their properties with those of PMN–33PT composition [8] which has a lower Curie temperature. Remanent polarisation, coercive field, piezoelectric constants and non linear dielectric properties under high ac electric field were measured and then compared with those of PMN–PT and PZT ceramics [9,10].

2. Ceramics by conventional sintering & hot forging

PIN–PT, PIN–PMN–PT ceramics were synthesised by two steps solid state reaction via Wolframite and Columbite phases. The Wolframite ($InNbO_4$) or Columbite ($MgNbO_4$) was formed by In_2O_3 or Mg_2O_3 with Nb_2O_5 at 1100 °C for 24 h. The intermediate oxides were then mixed with PbO and TiO_2 and ball-milled with Zirconium micro bead ($\sigma < 1.6$ mm) using continuous attrition milling setup (Labstar). The mixtures were dried and calcined at

* Corresponding author. Tel.: +33 1 69 41 58 88.
E-mail address: mai.phamthi@thalesgroup.com (M. Pham-Thi).

0041-624X/$ - see front matter © 2006 Published by Elsevier B.V.
doi:10.1016/j.ultras.2006.05.017

850 °C for 2 h to form stoichiometric perovskites. The ultra fine perovskite powder, showing the submicronic grain size (Fig. 1a; $\sigma \sim 0.2$ μm), was obtained by re-milling. The green ceramics pellets with density about 50–60% of theoretic density were obtained by axial pressing. The green PIN–PT pellets were hot-forged at 1000 °C for 1 h under a pressure of 1 T/cm^2. The hot-forged ceramics were finally annealed under an O_2 flow at 1200 °C for 4 h. Yellow pale translucent ceramics with high relative densities (>98% $d_{\text{theoretical}}$) were achieved (Fig. 1b). Translucent PIN–PT ceramics show large ceramic grain size over ten microns and fine grain size about 1–2 μm (Fig. 1c). Dense ternary PIN–PMN–PT ceramics (>98% d_{theo}), obtained using conventional sintering, show fine and uniform grain size about 2 μm. XRD spectra of both powder and ceramic show only a single-phase perovskite.

3. Electromechanical properties

Samples were cut in discs (10 mm × 0.5 mm), plates (10 × 2 × 0.5 mm^3) and bars (10 × 2 × 1.5 mm^3). Silver paste was painted on the polished faces and fired at 700 °C during 30 min.

PIN–PT samples were poled in a silicon oil under a 4000 V/mm field at room temperature during 10 min whereas ternary PIN–PMN–PT and PMN–PT samples were poled under a 400 V/mm field at 200 °C and then cooled down to 50 °C under the same field. The temperature dependence of the dielectric constant was measured at 1 kHz using a HP 4192A impedance analyser. Hysteresis loops measurements were made using a Tower-Sawyer set-up using triangle burst waves at 0.1 Hz. Electromechanical properties were measured according to the IRE standard method with an Agilent 4294A impedance analyser.

Table 1 resumes all the electromechanical constants at low level (0.5 V) for the compositions xPIN–yPMN–zPT, PIN–37PT and PMN–xPT [8]. Fig. 2 presents the temperature dependence of the dielectric constant ($\varepsilon_{33}^T/\varepsilon_0$) and the radial coupling coefficient (k_p) for PIN–37PT, PMN–33PT, PMN–36PT and the two studied ternary compositions.

The dielectric curves, obtained at 1 kHz, present maxima at $T_{\max}$ (Fig. 2a) corresponding to the well known

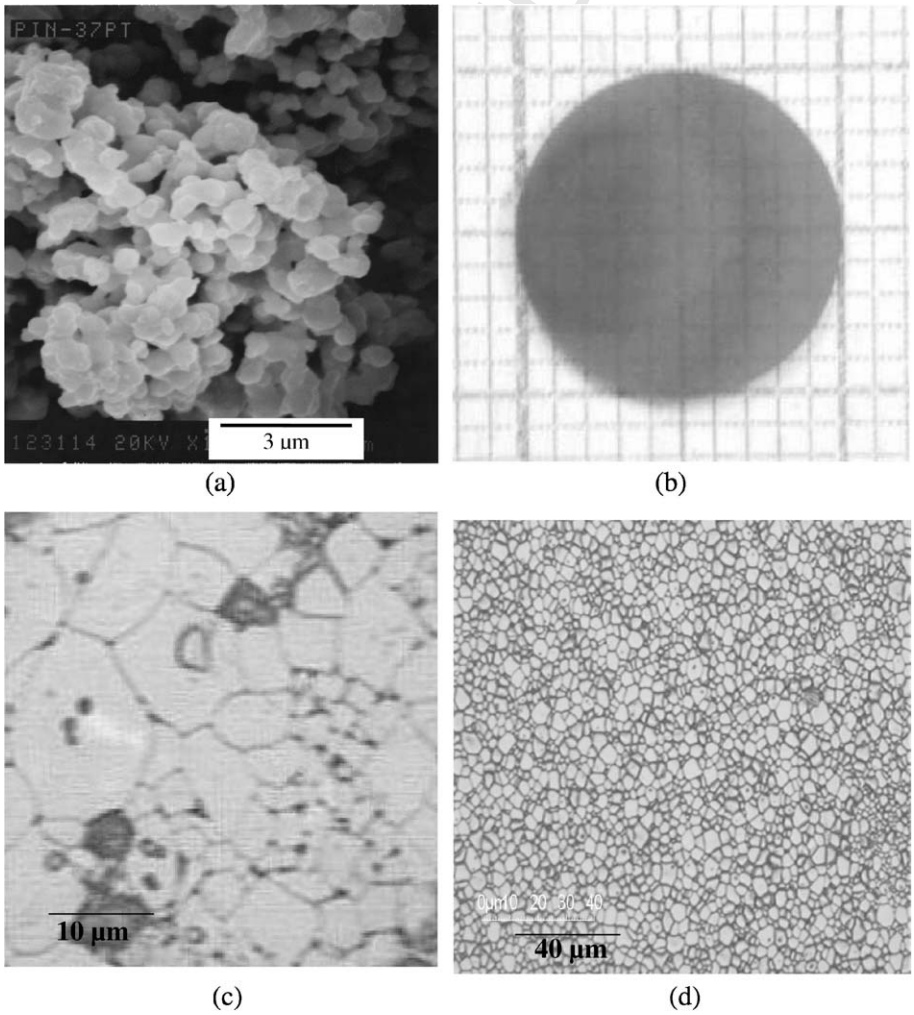

Fig. 1. Photographies of PIN–PT perovskite powder (a), PIN–PT translucent ceramic (b), microstructure of PIN–PT (c) and PIN–PMN–PT (d) ceramics.

Table 1
Dielectric and electromechanical properties of PIN–PMN–PT, PIN–PT and PMN–PT [8] ceramics

Properties	PIN–37PT	16PIN–51PMN–33PT	24PIN–42PMN–34PT	PMN–33PT	PMN–36PT
$\varepsilon_{33}^T/\varepsilon_0$@1kHz	2672	2420	3100	2920	4830
k_{33}	0.623	0.71	0.72	0.69	0.63
d_{33} (pC/N)	428	416	496	453	499
d_{33}Berlincourt (pC/N)	413	*	*	*	*
s_{33}^E (pm^2/N)	15	16	17	16	15
$M_{33} = (d_{33}/s_{33}^E)^2$ (C^2/m^4)	812	676	841	784	1089
$d_{33}\varepsilon_0/\varepsilon_{33}^T$ (pC/N)	0.160	0.172	0.16	0.155	0.103
Q_m	53	90	74	124	121
k_{31}	0.36	0.35	0.41	0.34	0.29
d_{31} (pC/N)	−193	−189	−230	−186	−217
s_{11}^E (pm^2/N)	14	11	12	12	14
Q_m	76	110	91	*	*
k_p	0.57	0.62	0.61	0.58	0.52
Q_m	71	90	105	*	*
k_t	0.47	0.50	0.48	0.50	0.42
Q_m	71	100	140	*	*
$\varepsilon_{11}^T/\varepsilon_0$@1kHz	1716	2350	2500	2311	3105
k_{15}	0.51	0.53	0.52	0.40	0.50
d_{15} (pC/N)	368	455	468	276	470
s_{55}^E (pm^2/N)	34	49	36	30	37
Q_m	41	60	60	*	*

tetragonal-cubic phase transition. As expected, T_{max} increases from 175 to 180 °C, 195 and 290 °C, respectively for PMN–33PT, ternary and PIN–37PT [7] compositions, i.e., for the ceramics with increasing PIN concentration. The dielectric curves present another anomaly due to the rhombohedral–tetragonal or monoclinic–tetragonal phase transition. This ferroelectric–ferroelectric transition takes place towards 90 °C for the 24PIN–42PMN–34PT and 120 °C for 16PIN–51PMN–33PT. This anomaly is less marked for PIN–37PT and is observed towards 80 °C for the PMN–33PT.

PMN–36PT and PIN–37PT ceramics exhibit nearly the same radial coupling coefficient at RT (Fig. 2b). PMN–36PT ceramics show a decrease of the coupling coefficient from RT ($k_p = 0.55$) to 60 °C, then a continuous decrease up to 160 °C ($k_p = 0.38$) and a drop at 185 °C. This behaviour is consistent with the observed phase transitions of PMN–36PT ceramics: ferroelectric–ferroelectric transition around 80 °C and ferroelectric–paraelectric transition at 180 °C [4]. Ternary compositions exhibit a higher k_p at RT that remains constant up to 85 °C, the temperature of the ferroelectric–ferroelectric transition, then decreases continuously up to 148 and 160 °C before dropping and reaching plateau at 170 and 190 °C, respectively for 16PIN–51PMN–33PT and 24PIN–42PMN–34PT. It is worth noting that PIN–37PT ceramics exhibit only slight decrease of k_p from RT ($k_p = 0.55$) up to 200 °C ($k_p = 0.41$).

The electromechanical properties at low level (0.5 V) of PIN–37PT are comparable with those of PMN–PT set apart piezoelectric d_{ij} constants for which PMN–36PT presents much more important values. Among the two studied ternary compositions, 24PIN–42PMN–34PT presents the best dielectric and electromechanical properties (Table 1). The dielectric constant at room temperature, $\varepsilon_{33}^T/\varepsilon_0$@1kHz = 3100, is intermediate between those of PIN–37PT and PMN–36PT. The electromechanical properties of ternary ceramics are comparable to those of PMN–PT ceramics, the difference of dielectric constants being compensated with the higher electromechanical coupling coefficients.

4. Non linear properties

Drift measurements or ac electric field dependences of the dielectric constant were measured up to 1 kV/mm. Sinusoidal signal at 1 kHz, generated from a HP 3314 A function generator, was amplified by a Kepco Bipolar Amplifier. A EG& G 5210 Lock-in Amplifier and an integration capacitance (C_i) allow to measure the capacitance (C) at the sample connexions.

All materials show relatively square hysteresis loops (Fig. 3). The coercive fields (E_c) of ceramics containing PIN are much higher than those in PMN–PT ceramics (Table 2) and the remanent polarization (P_r) is also higher: this indicates a harder material than PMN–PT which is consistent with the higher Curie temperatures. E_c and P_r increase with the increasing PT or PIN concentrations. E_c reaches 710 V/mm for PMN–36PT and 1660 V/mm for PIN–37PT. At the same time, P_r reaches 0.344 C/m^2 for PIN–37PT but 0.29 and 0.45 C/m^2, respectively for PMN–33PT and PMN–36PT. The two ternary compositions present intermediate E_c and P_r between those of PMN–PT and PIN–PT.

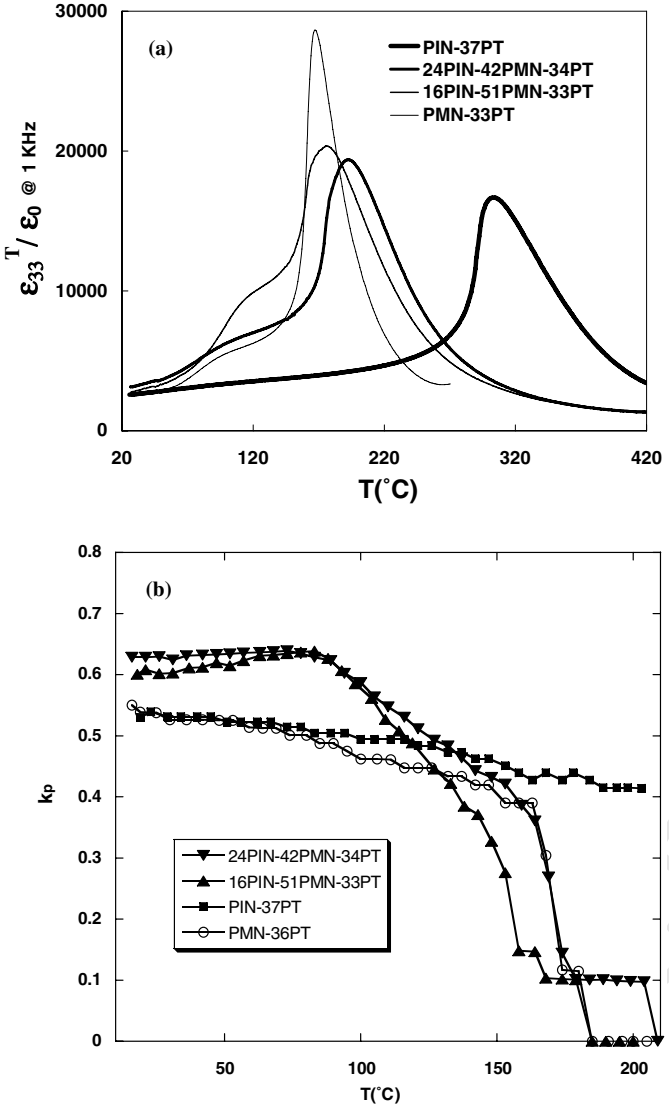

Fig. 2. Temperature dependence of the dielectric constant $\varepsilon_{33}^T/\varepsilon_0$@1kHz (a), and radial electromechanical coupling coefficient of PMN–PT, PIN–PT and PIN–PMN–PT ceramics (b).

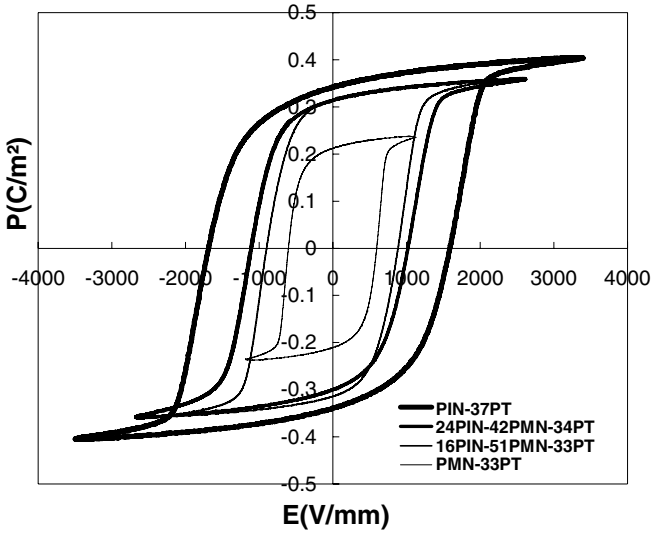

Fig. 3. Hysteresis loops of PMN–PT, PIN–PT and PIN–PMN–PT ceramics.

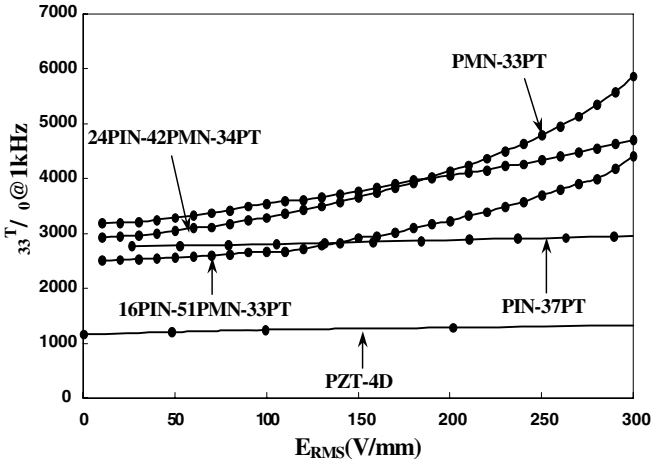

Fig. 4. Ac electric field dependence of the dielectric constant $\varepsilon_{33}^T/\varepsilon_0$@1kHz for different poled ceramics.

The ac electric field dependence of the dielectric constant $\varepsilon_{33}^T/\varepsilon_0$@1kHz for poled ceramics are reported in Fig. 4. All ceramics present linear drift: the dielectric permittivity $\varepsilon_{33}^T/\varepsilon_0$ increases linearly with the ac applied electric field (E_{ac}). It is related to some motions of the ferroelectric domain walls under the electric field. This is generally known as the ''extrinsic contribution''. This linear drift is observed up to 300 V/mm for PIN–37PT and typical hard PZT–4D material while 24PIN–42PMN–34PT, 16PIN–551PMN–33PT and PMN–33PT exhibit linear drift up to 250, 150 and 120 V/mm. Above those fields, the latter ceramics show an accelerated drift behaviour: the permittivity increases very abruptly with the applied electric field. This thermal runaway phenomenon due to the increase of dielectric losses is in agreement with the observed low T_C. The higher the Curie temperature is, the higher is the required electric field to switch the polarization between adjacent ferroelectric domains. Therefore, the linear-drift

Table 2
Curie temperature, coercive field and remanent polarisation of PMN–PT, PIN–PT and PIN–PMN–PT ceramics

	PMN–33PT	PMN–36PT	16PIN–51PMN–33PT	24PIN–42PMN–34PT	PIN–37PT
T_C (°C)	160	180	180	195	300
E_C (V/mm)	580	710	890	1020	1660
P_r (C/m^2)	0.29	0.450	0.316	0.314	0.344

region for PIN–37PT and PZT–4D is larger than that for ceramics containing PMN, and the accelerated drift region is not observed.

The linear drift can be characterized by the Rayleigh coefficient: $\alpha_{ac}^{T} = \frac{1}{\varepsilon_{33_0}^{T}}\left(\frac{\partial \varepsilon_{33}^{T}}{\partial E_{ac}}\right)$. As expected, the Rayleigh coefficients of PIN–37PT and PZT–4D have the same value, $\alpha = 3.4$, and increases to 17.2, 27.4 and 33.4 for ternary and PMN–33PT ceramics.

5. Conclusions

Among PIN–xPT compositions, PIN–37PT presents the best dielectric and electromechanical properties at low level [5]. Such a behaviour is characteristic of morphotropic compositions. The important values of ε_{ij}^{T}, s_{ij}^{E}, d_{ij} and the low Q_m values of PIN–37PT are characteristic of a soft material.

The electromechanical properties of PIN–37PT are comparable to those of PMN–PT except lower dielectric and piezoelectric d_{ij} constants. The dielectric constant at room temperature is directly related to the Curie temperature: generally, the more the Curie temperature is raised, the lower is the dielectric constant at room temperature. PIN–37PT presents a Curie temperature $T_C = 300°C$ higher than that of PMN–36PT, $T_C = 180$ °C. Its dielectric constant and thus its piezoelectric constants at room temperature are lower than those of PMN–36PT. The incorporation of PIN in PMN–PT ceramics results in an increase of structural transition temperatures and thus a decrease of the dielectric constant at room temperature.

The electromechanical properties of ternary ceramics are similar to those of PMN–PT ceramics, the difference between dielectric constants being compensated by the higher electromechanical coupling coefficients.

The temperature dependence of the planar electromechanical coupling coefficient shows that the higher the Curie temperature is, the better is the stability of k. Therefore, the higher the ferroelectric–ferroelectric temperature transition is, the more the decrease of k is delayed. These same tendency should be observed for the other electromechanical constants.

Our purpose is thus to synthesise materials having structural transition temperatures high enough to delay the drop of the electromechanical properties when temperature is increased. However, power applications require high dielectric and piezoelectric constants. From this point of view, PIN–PMN–PT ceramics seem to be a good candidate.

References

[1] Y.H. Chen, K. Uchino, J. Appl.Phys. (2001) 3928–3933.
[2] Y. Hosono, Y. Yamashita, H. Sakamoto, N. Ichinose, Jpn. J. Appl. Phys. 42 (2003) 5681–5686.
[3] N. Yasuda, S. Shibuya, J.Phys.: Condens. Matter 1 (1989) 10613–10617.
[4] Y. Yamashita, K. Harada, Y. Hosono, S. Natsume, N. Ichinose, Jpn. J. Appl. Phys. 37 (1998) 5288–5291.
[5] Y. Hosono, Y. Yamashita, H. Sakamoto, N. Ichinose, Jpn. J. Appl. Phys. 42 (2003) 535–538.
[6] E.F. Alberta, A.S. Bhalla, J. Phys. Chem. Solids 63 (2002) 1759–1769.
[7] C. Augier, M. Pham-Thi, H. Dammak, P. Gaucher, J. Eur. Ceram. Soc. 25 (2005) 2429–2432.
[8] H. Hemery, Ph.D thesis, Céramiques orientées hautes performances: $Pb(Mg_{1/3}Nb_{2/3})O_3$–$PbTiO_3$ par croissance pseudo-morphose, INSA Lyon France (2003).
[9] Mai Pham Thi, Henri Hemery, Ph. Colomban, Olivier Lacour, 14th IEEE International Symposium on Applications of Ferroelectrics, ISAF (2004) 157–160.
[10] P. Gonnard, M. Pham-Thi, International Symposium on Applications of Ferroelectrics, ISAF (2004) 51–55.